The Effect of Controlled Thermo Mechanical Processing on the Properties of a High Strength Steel

*M. Heydarian**
Industrials Organization, Isfahan, Iran

Abstract

In this paper, an ultra low carbon High Strength Low Alloy Grade Steel was subjected to a two-step forging process and this was followed by different post cooling methods. The highest strength was obtained at a faster cooling rate due to the highly dislocated acicular ferrite structure with the fine precipitation of microalloying carbides and carbonitrides. At a slow cooling rate, the strength fell with an increase in ductility due to the larger volume fraction of the less dislocated polygonal ferrite structure. The strength remained almost unchanged with a further decrease in the middle cooling rate due to the formation of a predominantly polygonal ferrite microstructure. At the slower post cooling rates, a high impact toughness value was obtained at the ambient temperature and at -40°C testing temperature; this was due to the fine grained polygonal ferrite microstructure. At all post cooling methods, the change in the impact toughness value at the ambient temperature and at the temperature of 40°C was found to be negligible due to the ultra-low carbon content of the steel.

*Keywords:*Thermo Mechanical Processing, Forging, Mechanical Properties, Microstructure.

1. Introduction

The development of low carbon, copper bearing, precipitation strengthened high strength, low-alloy (HSLA) plate steel has been a key element of the U.S. Navy's efforts to reduce the shipbuilding costs. HSLA-100 and HSLA-80 grade steels are Cu bearing low carbon steels developed by the US navy in the mid-1980s [1]. The continuous cooling transformation behaviors of these types of steels have been explored by the earlier studies [2–4]. The microstructural characterization of as rolled and tempered HSLA-100 steels has been reported [5–7]. The structure and properties of these steels at various processing conditions have also been studied by the previous researchers [8–10].

However, in most cases, the steels were processed in rolling route, either by direct quenched (DQ) technique or under rolled– quenched (RQ) conditions [9,10]. On the other hand, another processing route, i.e. forging, has also been established as an alternative route to rolling in the processing of microalloying steels [11]. Forging route derives advantages of structural homogeneity and better soundness due to the application of isotropic deformation. Previous attempts by the present authors have been directed towards the development of HSLA forging using primarily HSLA-80 grade steels. It has been reported that variation in post-cooling rate engenders a variety of microstructures altering the strength properties significantly [12,13]. Later, newer alloy designs were introduced and the carbon content of the steels was reduced to 0.006 wt.% for better weldability and corrosion resistance. It has been found that a substantial amount of strength along with a negligible difference of toughness value at the ambient temperature and at -40 °C can be obtained by the application of a two-stage forging operation [14]. The dislocation substructure, along with fine microalloying precipitates that resulted from thermo mechanical controlled processing, was found to be mainly responsible for achieving high strength level and toughness of such ultra-low carbon HSLA steel.

The effects of cooling rates on the structure and properties of HSLA-100 or HSLA-80 grade steels have been reported elsewhere [15,16]. However, the effect of cooling rates on the ultralow carbon HSLA-100 grade steel has not been much explored.

In the present study, the carbon content of a HSLA-100 grade steel was lowered to 0.005 wt.% and a two-stage controlled forging operation was applied. Subsequently, the forged slabs were cooled in different cooling media. The present study evaluated the structure and the properties of some ultra-low carbon steel processed by this forging technique.

2. Experimental procedure

In this investigation, some ultra-low carbon steel

**Corresponding author*
Email: ZOLAL1363@gmail.Com
Addrees: Industrials Organization, Isfahan, Iran
M.Sc.

Table 1. Chemical composition of the steel (wt.%).

V	Al	Ti	Nb	P	S	Si	Mo	Cr	Mn	Cu	Ni	C
0.005	0.02	0.01	0.05	0.006	0.009	0.28	0.55	0.57	1.23	2.1	3.50	0.005
C.E=C+(Mn+Si)/6 +(Ni+Cu)/ 15+(Cr+Mo+V)/ 5=0.85												

was melted in an air induction furnace and cast in a metal mould. The chemical composition of the steel, as analyzed in Quantovac and LECO, is shown in Table 1. Ingots of 50-50 mm cross section were reheated at 1200 °C for 2 h. Forging was carried out in a one-ton capacity down stroke power hammer in two stages. In stage I, 50% deformation was achieved by six repeated strokes in the temperature range of 1100–1050 °C to reduce the cross section of the slab to 35-35 mm. In Stage II, another 50% deformation was achieved by similar six repeated strokes in the temperature range of 850–800 °C to obtain the final cross section of 25-25 mm. Subsequently, the forged slabs were subjected to water quenching (WQ), air cooling (AC) or sand cooling (SC). Temperatures at different stages of forging and during cooling were measured by thermocouples inserted into the forged bars and also, by infrared pyrometer (MINOLTA/LAND-52 CYCLOPS-52).

Optical metallographic samples prepared by conventional grinding and polishing techniques were etched with 2% nital solution and observed by a light microscope. Thin foils for transmission electron microscopy (TEM) were prepared by twin jet polishing in an electrolyte of 90% acetic acid and 10% perchloric acid. Thin samples were observed in a Transmission Electron Microscope (Philips CM200 with EDAX) at 200 kVoperating voltage. The chemical compositions of precipitates were determined by energy dispersive X-ray (EDS). Tensile testing was carried out in an Instron tensile testing machine (Model No. 4204) by keeping a constant cross head speed of 8.3×10^{-3} mm/s. Standard impact specimens (ASTM; vol. 03.01: E23–96) were prepared and Charpy impact testing was carried out at room temperature and -40 °C.

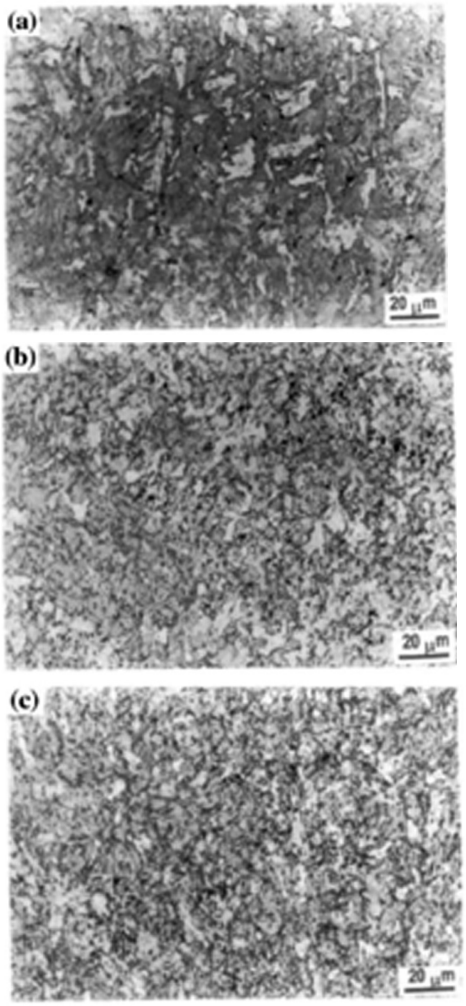

Fig. 1. Optical micrographs of the steel at different post-cooling rates:
(a) 35°C/s (water-quenched), (b) 1.15°C/s (air-cooled) and (c) 0.68°C/s (sand-cooled)

3. Results and discussion

3.1. Microstructure

The optical microstructures of the steel at various post-cooling conditions showed a mainly ferritic structure, as can be observed in Fig.1. An overall fine structure (2–5 μm grain size) was obtained in the steel at different cooling rates from a final forging temperature of 800 °C. Also the structural fineness was increased with increasing the cooling rate. The fine grain structure was due to the contribution of the second stage deformation in controlled thermomechanical processing. Prior austenite grain boundaries were not observed for any post-cooling conditions, as shown in Fig.1.

TEM examination showed an acicular ferrite structure at a faster cooling rate of 35 °C /s, as can be seen in Fig. 2a. At the cooling rates of 1.15 and 0.68 °C /s, the structure was a polygonal or quasi-polygonal ferrite, as can be seen in Fig.2b and c. Faster cooling from the 800 °C final forging temperature suppressed the formation of the polygonal ferrite and favored the formation of the acicular ferrite. The slower cooling rates of 1.15 and at 0.68 °C /s from the final forging temperature of 800 °C allowed sufficient time to pass into the high temperature transformation region of austenite. Hence, the diffusion of carbon was favorable at high temperature and facilitated the formation of the

polygonal or quasi-polygonal ferrite. It should be noted that Polygonal ferrite generally starts to nucleate at prior austenite grain boundaries and grows into the grains. Hence, a predominant polygonal ferrite structure resulted in the absence of prior austenite grain boundaries, as can be seen in Fig.1b and c.

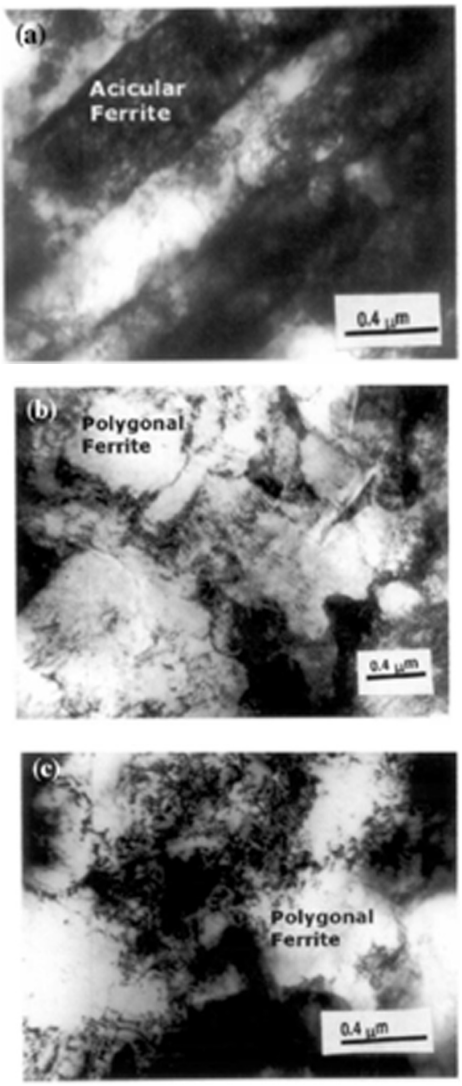

Fig. 2. Bright field TEM of the steel at different post-cooling rates:
(a)35 °C/s, (b) 1.15 °C/s and (c) 0.68 °C/s.

It is interesting to observe in optical micrographs (Fig.1) some dark particles are randomly distributed in the matrix; these are generally second phase particles as observed by earlier workers in low carbon and ultra-low carbon HSLA steels [2–14]. Krauss and his colleagues [2,3] have identified these second phase particles as martensite–austenite (MA) constituents or retained austenite, whereas Fonda and Spanos [17] have designated these particles as nonaligned second phase particles in ultra-low carbon steels.

It was interesting to observe that in optical micrographs (Fig.1), some dark particles were randomly distributed in the matrix; these were generally second phase particles as observed by the earlier workers in low carbon and ultra-low carbon HSLA steels [2–14]. Krauss and his colleagues [2,3] identified these second phase particles as martensite–austenite (MA) constituents or retained austenite, whereas Fonda and Spanos [17] designated these particles as nonaligned second phase particles in ultra-low carbon steels.

In the present investigation, TEM was employed to identify these second phase particles in this ultra-low carbon steel. At the magnified bright field image, a high dislocation density in the acicular ferrite lath was observed along with thin dark interlath regions, as shown in Fig. 3a. The dislocations in the acicular ferrite lath were found to interact with fine microalloying precipitates. The interlath dark regions became globular or chunky at 1.15 °C /s cooling rate and these particles were probably MA constituents, as can be seen in Fig. 3b. The magnified bright field image of air-cooled steel showed the twinned martensite in the interlath regions along with the inset selected area diffraction pattern (SADP), Fig.4a. The dark field was taken with the arrowed (101) twinned martensite spot, as shown in Fig. 4b. The separations of the twins were found to be 6–9 nm. The presence of the retained austenite in the interlath region of air-cooled steel was shown in the electron images, as can be seen in Fig. 5a and b. In the sand-cooled steel, similar types of globular or chunk-shaped second phase particles were observed and shown in the bright field image with inset SADP, as can be seen in Fig.6a. The dark field was taken with the arrowed (101) martensite spot, as shown in Fig. 6b.

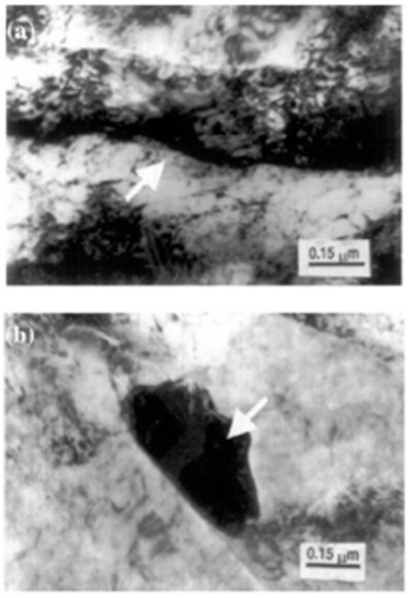

Fig. 3. Bright field TEM shows interlath dark particles (arrowed) at different cooling rates.
(a) 35 °C/s (b) 1.15°C/s.

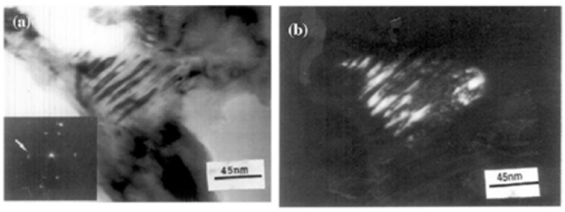

Fig. 4. TEM shows the twinned martensite in the interlath dark regions of the air-cooled steel: (a) the bright field with inset SADPand (b) the dark field.

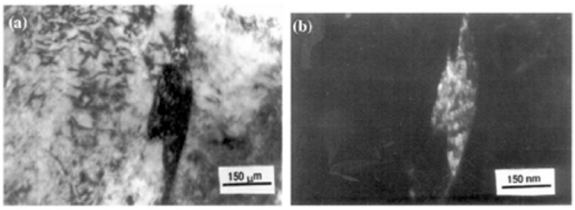

Fig. 5. TEM shows the retained austenite in the interlath dark regions of air-cooled steel: (a) the bright field and (b) the dark field with (002)γ reflection.

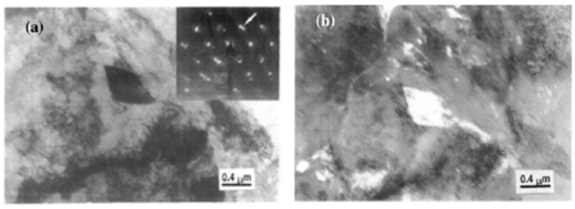

Fig. 6. TEM shows MA constituents in the sand-cooled steel: (a) the bright field with inset SADP and (b) the dark field.

It should be noted that this steel contains microalloying elements of Nb and Ti, which are well known as strong carbide formers. In low carbon steel, these microalloying elements form fine carbide and carbonitride precipitates, which enhance the strength of the steel [18,19]. It is obviously interesting to explore the precipitation behavior of such microalloying elements when the carbon content of the steel is 0.005 wt.%.

The bright field images of the steel cooled at 35 °C/s showed fine microalloying carbide and carbonitride precipitates 20–30 nm in size with regular geometric shapes in the dislocated acicular ferrite lath, as can be seen in Fig. 7a.

The precipitate size was increased at 1.15 °C/s post-cooling rate (25–45 nm in size) and their occurrence was mainly onto the dislocations, as can be seen in Fig. 7b and c. In the steel sand-cooled at 0.68 °C/s, these precipitates became larger in size (30–90 nm) and a low dislocation density was observed in the polygonal ferrite, as shown in Fig.7d. EDS analyses were performed for the cuboid or rectangular shaped particles; one of these is shown in Fig. 7e. From the EDS, it was found that that the precipitate was enriched with Ti, Nb and also, Cu. Hence, it can be concluded that it is a complex type of precipitate which combines Ti/Nb carbide or carbonitride along with Cu.

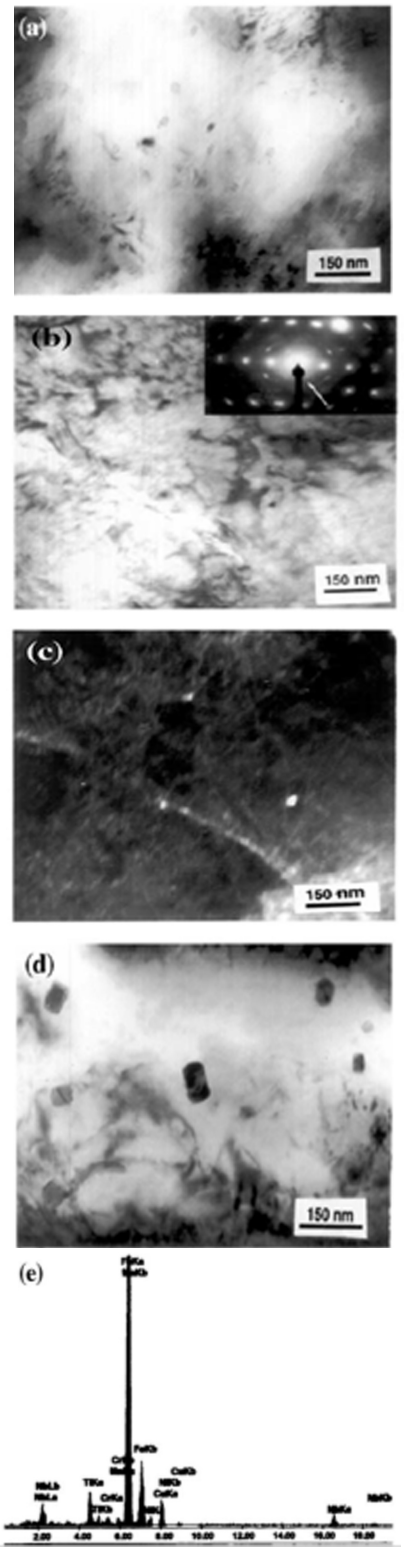

Fig. 7. TEM shows precipitates in the steel at different post-cooling rates: (a) the bright field at 35 °C/s, (b) the bright field with SADP inset at 1.15 °C/s, (c) the dark field of (b) with arrowed precipitate spots in SADP, (d) the bright field at 0.68 8C/s and (e) EDS from a precipitate.

3.2. Mechanical properties

The effect of cooling rate on the tensile properties of the steel is shown in Fig. 8. The UTS and YS values obtained in water-quenched steels were 974 and 888 MPa, respectively, which were well above the commercial HSLA-100 grade steel 1). The strength value was dropped to 863 MPa UTS and 704 MPa YS on air cooling. However, the percentage of elongation in air-cooled steel was increased from the 15.3% value observed for the water-quenched steel to 19.1%. The strength values were changed marginally when the post-cooling rate was further decreased to 0.68 °C/s.

The UTS and YS values obtained in sand-cooled steel were 868 and 726 MPa, along with 21.4% elongation.

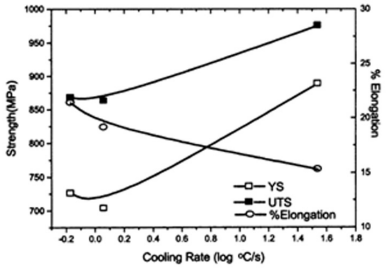

Fig. 8. The effect of the cooling rate on the tensile properties of the steel.

The high strength in water-quenched steel was mainly due to the fine grain structure obtained by the controlled forging operation and the highly dislocated acicular ferrite structure obtained at rapid cooling from the 800 °C final forging temperature. The strength value was dropped on slower cooling in air or sand air cooling due to the predominantly polygonal ferrite structure which contained a lower less dislocation density and coarsened microalloying precipitates.

The effects of the cooling rate and impact toughness values at ambient and sub-ambient temperatures are shown in Fig. 9. For the air-cooled steel, the room temperature toughness was 175 J and it was dropped slightly to 158.15 J at -40 °C, as shown in Fig. 9. The ambient temperature toughness value was nearly 33% lower for the water-quenched sample compared to that of the air-cooled sample. No significant change in toughness was observed between air and sand-cooled steel at ambient and sub-ambient temperatures.

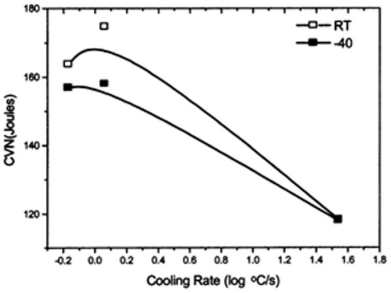

Fig. 9. The effect of the cooling rate on the impact toughness of the steel.

The most interesting result found in this study was related to the observation that the toughness of this steel remained almost unchanged from ambient temperature to -40 °C for different post-cooling conditions due to the ultra-low carbon content of the steel. The fine-grained polygonal ferrite structure obtained by controlled thermo-mechanical processing resulted in a high toughness value at the slower cooling rates. A comparatively lower toughness value at the higher post-cooling rate could be due to the predominantly acicular structure in the steel.

4. Conclusions

The following conclusions can be drawn from the present study:

1. By applying controlled thermo-mechanical processing, a fine-grained structure was obtained in this steel. The transformation product obtained at a fast post-cooling rate (water cooling) was a predominantly acicular ferrite. The microstructure was changed to a polygonal or quasi-polygonal ferrite when the cooling rate was slowed down to 1.15 or 0.68 °C/s by air or sand cooling, respectively.
2. The strength level obtained at the faster cooling rate of 35 °C/s was 974 MPa UTS and 888 MPa YS, respectively, along with 15.3% elongation. This high strength level was obtained due to the highly dislocated acicular ferrite structure along with the fine precipitation of microalloying carbides/carbonitrides. The strength value was dropped to 863 MPa UTS and 704 MPa YS at a slower cooling rate of 1.15 °C/s with an increase in ductility (19.1% elongation). The less dislocated polygonal ferrite structure obtained at the slower cooling rate decreased the strength value with an increase in ductility. The strength value remained almost unchanged with a further decrease in the cooling rate to 0.68 °C/s as the predominant microstructure remained the polygonal ferrite.
3. At slower post-cooling rates, high impact toughness values were obtained at ambient temperatures and at -40 °C due to the formation of a polygonal ferrite microstructure. Due to the ultra-low carbon content of the steel, the difference in impact toughness values at ambient and at -40 °C temperature was found to be negligible for steels cooled in air or sand.

References

[1] C. Zyryca: Eng. Mater., 85(1993), 490.
[2] T. hompson, S. Colvin, D. Krauss: Metal. Trans. A Phys. Metal. Mater. Sci., 21(1990), 1392.
[3] T. hompson, SW. Colvin, DJ. Krauss: Metall. Mater. Trans. A Phys. Metal. Mater Scie., 27(1996), 1452.
[4] D. unne, S. Ghasemi, S. Banadkouki: ISIJ Int,. 36(1996), 324.
[5] R. Varughese, R. Howell: Mater. Charact., 30(1993), 352.

[6] D. Wenpu, D. Zuobao, F. Lang: Mater. Charact., 37(1996), 158.
[7] M. Miglin, J. Hirth, P. Rosenfield: Metall Trans A Phys. Metall. Mater. Sci., 17(1986), 789.
[8] M. Mujahid, M. Lis, K. Garcia, I. DeArdo: Mater Eng., 7(1996), 247.
[9] J. Yoo, J. Choo, W. Park, T. Kim: ISIJ Int., 35(1995), 1034.
[10] G. Hwang, G. Lee, S. Yoo, J. Choo: Mater. Sci. Eng. A , 25(1998), 198.
[11] G. Krauss, G. Banerji: Fundamentals of micro alloying forging steels. The Metallurgy Society Inc , Oxford (1988), 158.
[12] S. Das, S. Ghosh, A. Kundu, S. Chaterje: Trans. Indian. Inst. Met , 56(2002), 24.
[13] S. Das, S. Ghosh, A. Chatterjee, S. Ramachandra: Mater. Charact., 50(2002), 299.
[14] S. Das, S. Ghosh, A. Chatterjee, S. Ramachandra: Scand. J. Metal., 33(2004), 198.
[15] S. Dhua, S. Mukerjee, D.Sarma: Metall. Mater. Trans , 34A(2003), 405.
[16] S. Das, S. Ghosh, A. Chatterjee, S. Ramachandra: Scr. Mater., 7(2003), 48.
[17] R. Fonda, R. Spanos: Metall. Trans. A. Phys. Metall. Mater. Sci., 32A(2001), 219.
[18] B. Dutta, B. Valdes, E. Sellars: Acta. Met., 40(1992), 653.
[19] A. DeArdo: ISIJ Int., 35(1995), 946.